Large datasets from artificial intelligence exploration of unstable oil-droplet model protocells allow prediction of properties and collective behaviour

Laurie J. Points[1], James Ward Taylor[1], Jonathan Grizou[1], Kevin Donkers[1], Leroy Cronin[1*]

[1]WestCHEM, School of Chemistry, University of Glasgow, Joseph Black Building, University Avenue, Glasgow G12 8QQ, U.K. [*]Corresponding author email: Lee.Cronin@glasgow.ac.uk

Contents

Supplementary Methods

Robotic Hardware

The robotic platform used within this work is based upon that previously reported by this group.[1] Summarised here are the modifications to the robotic hardware undertaken during this work. The only significant modifications to the platform were those undertaken to allow the use of multiple aqueous phase constituents.

Robot Frame

The robot frame design was similar to the previously used robotic platform, but the external dimensions were reduced from 54 × 42 cm to 42 × 42 cm. The interior dimensions were therefore reduced from 46 × 34 cm to 34 × 34 cm. This resulted in a shorter belt length and better reliability in carriage movement.

Liquid Handling

Instead of a single aqueous phase being dispensed by a single syringe pump, multiple different aqueous phases had to be dispensed, using either a valve to select between bottles of aqueous phase connected to a syringe pump, or by using four syringe pumps to dispense one solution each. In the first implementation of a system where the aqueous phase could be varied, two syringe pumps each connected to a six-way rotary valve were used in order to pump six different aqueous phases (three each), plus deionised water for washing. When using the valves, 6-position selection valves for 1/16" OD tubing (Upchurch Scientific, part #V-240) were placed in an enclosure of in-house design and build and driven by a stepper motor. The electronics consisted of an Arduino Mega 2560 with Marlin firmware to control the XY carriage and servos, connected via a serial interface to another Arduino Mega 2560 that controlled the pumps and valves. Further details of the electronics can be found in the hardware and software manual published previously.[2] In the second implementation, where each aqueous phase had its own dedicated pump for delivery, Tricontinent C3000 syringe pumps were controlled directly from the control PC's serial port.

Software Implementation

The software implementation was very similar to that of the previous work on evolution of oil droplets, with Python 2.7 handling the genetic algorithm and random experiment generator, passing the formulations to be tested to the robot controller which communicated with the robot Arduino via a serial port, which was written in C++. Minor changes were made to way the robot controller handled the experiments to allow for easier variation of experimental procedure and experiment generation algorithm.

Proximity Limited Random Search

The parameter space generated by 6 surfactants and 4 oils (1.8×10^{20} combinations, based on 4 oil inputs with 70 increments, and 6 aqueous phases with 140 increments) is so large that neither a lattice search nor a purely random search would have been an effective technique to search the space. If a lattice search was performed using the same parameters as for the previous oil phase only system, 1,048,545 unique recipes would have to be tested, compared to the 225 needed for the oil only system, to achieve the same level of coverage. Therefore a proximity limited random search was performed. Random points in the space were generated, each corresponding to an experiment. However, the points were only used if they were of a sufficient distance from each other. For this project we tested 393 random, proximity limited points over the whole 10 dimensional space. This allowed a broad screening of the space within an experimentally achievable timeframe.

Algorithm

1. Calculate proximity threshold from number of oils and surfactants
   proximity_threshold = $\sqrt{n_{oils} + n_{surfactants}}$ × threshold_factor
2. For 100 attempts:
   2.1. Generate array of random numbers (length oils + surfactants)
   2.2. Compare new array proximity to all previous arrays
   2.3. If proximity larger than proximity_threshold:
      2.3.1. Add array to history
      2.3.2. Return array
   2.4. If not, repeat from 2.1
3. If array cannot be found outwith proximity_threshold (this did not occur during the experiments):
   3.1. Return last array
   3.2. Return message stating proximity condition not met

A threshold_factor of 0.20 was used for a space of 10 dimensions (4 oils + 6 surfactants).

The total possible number of combinations for the space was calculated using the formula:

$$N = \left(\frac{Oil\ vol\ (mL)}{Oil\ precision\ (mL)}\right)^{Number\ of\ oils} \times \left(\frac{Aqueous\ vol\ (mL)}{Aqueous\ precision\ (mL)}\right)^{Number\ of\ aqueous}$$

Genetic Algorithm

The genetic algorithm used in this work was identical to that used in our previous work. To explain briefly, 24 random combinations were tested (generation 0), and the fitness factors evaluated by the image tracking software. “Roulette wheel” selection was then used, with formulations giving a higher fitness having a higher probability of being selected to breed into new individuals. The top 20 were crossed over with each other and mutated at random points by a random mutation factor to give the next generation of 10 formulations to be tested. This process was repeated for 30 generations.

Parameter	Oil Only	Aqueous Only	Combined	6 Aqueous
Genome Length	4	4	8	10
Population Size	25	24	24	24
Carry-overs	15	14	14	14

Per-locus mutation rate	0.3	0.3	0.3	0.3
QTL mutation (SD)	0.1	0.1	0.1	0.1
Selective pressure	1	1	1	1

Supplementary Table 1 - Genetic algorithm parameters used for evolutionary optimization experiments.

Reproducibility

The top four fitness formulations from each GA run were repeated 8 times each, and their movement fitness was measured. The mean fitness over the 8 repeats was compared to the original measured fitness during the GA run. There was a range of reproducibility, with four of 12 formulations from the 8 parameter GA reproducible to within 1.0 mm s^{-1} of the original value. All but two were within 1.5 mm s^{-1} of the original value (a difference of <30 %) (Supplementary Table 8). The reproducibility for the aqueous only optimized formulations was more variable, with only half of the tested formulations giving mean fitness values within 50% of the original determined fitness. The lower original fitness overall meant that instances resulting in very low fitness due to interaction with the walls or other droplets had a more marked effect on the mean over 8 repeats. It is thought that much of this variability is due to seasonal temperature variation in the lab, with temperature control being implemented for subsequent experiments.

Experimental Procedures

Manual Procedures

Oil and Aqueous Phase Preparation

All surfactants and oils used in this work were purchased from Sigma-Aldrich Corporation. Due to the need for maximum consistency throughout experiments, standard operating procedures were developed for oil and aqueous phase preparation which are shown here.

Preparation of surfactant solutions – Standard Operating Procedure

All surfactant solutions were prepared fresh before each experimental run, thus ensuring that any pH variation during the run (for example due to absorbing CO_2 from the air) was consistent for each run. The consistency of the pH was also checked by measuring the pH at the end of each experimental run.

1. Weigh out the required amount of surfactant/modifier into a beaker.
2. Add distilled water and stir using a glass rod to dissolve.
3. Transfer the resulting solution to a 5 L plastic bottle with a mark at 5 L.
4. Repeat steps 2 and 3 until complete transfer of material to the bottle is achieved, taking care to leave space to adjust pH.
5. Ensure the pH meter is calibrated using buffers 10 and 13.
6. Add 5 M $NaOH_{(aq)}$ solution until desired pH is reached.
7. Make up the solution with distilled water until close to the mark.
8. Mix well by closing the lid and shaking the bottle.
9. Allow the solution to equilibrate to the temperature of the lab used for experiments and for any bubbles to settle.
10. Adjust the to the desired pH using 5 M $NaOH_{(aq)}$.
11. Make up to the 5 L mark with distilled water.

	TTAB	Triton X-100	PEG-400	DDMAB	CTAB	Brij O-10
pH (Target, ±0.1)	12.70	12.30	13.05	12.75	13.00	13.00

Supplementary Table 2 - Surfactant solution target pH values.

Preparation of Oil Formulations – Standard Operating Procedure

1. Measure required oil quantities into a 200 mL bottle using a measuring cylinder.
2. Weigh out 0.25 $mgmL^{-1}$ Sudan III
3. Add the Sudan III to the mixture.
4. Shake well to ensure the dye is dissolved.

Surfactant screen

When choosing which surfactants to include in our increased parameter space, we wanted to ensure that we had surfactants with a wide range of properties. As such, a surfactant screen was undertaken which included anionic, cationic, non-ionic and zwitterionic surfactants. A 20 mM aqueous solution of each of these surfactants was prepared and taken to pH = c. 13 using 5 M $NaOH_{(aq)}$ and tested with three highly evolved oil formulations (one for each of movement, vibration and division) previously reported. Through both qualitative observation and analysis by fitness functions, the surfactants were seen to have a range of effects on the droplet behaviours. In some cases the highly evolved behaviours were observed, in some cases other behaviours were observed and in some cases stationary droplets, droplets that stuck to the sides or oil slicks were observed. Given this information, six aqueous phase modifiers were chosen for use on the automated platform: the cationic surfactants TTAB and CTAB; the non-ionic surfactants Brij O10 and Triton X-100; the zwitterionic surfactant DDMAB and poly(ethylene glycol) (Mn = 400).

Bulk Property Measurement

All manually prepared solutions were prepared from the bulk aqueous phases / dyed oils used on the robotic platform, with the desired oil quantities measured out using a displacement pipette. Oil phases were then vortexed to mix whilst aqueous phases were shaken or stirred (depending on the volume prepared) and left for the bubbles to settle. The surface tension of oil and aqueous phases were measured using a Lauda TD-1C Ring/Plate tensiometer using the EZ141Du Noüy ring attachment, calibrated using a 500 mg weight. Surface tension measurements were all measured in at least triplicate. The density, kinematic and dynamic viscosities of the oil and aqueous phases were measured using an Anton Paar Stabinger Viscometer SVM 3000/G2 with a set temperature of 20 °C, using method M6 repeat standard measurement.

pH Indicator Work

Experiments using phenolphthalein pH indicator were undertaken using the same method as other automated experiments, but with the set of formulations used predefined by the operator rather than being generated by a genetic algorithm. 0.002 gmL^{-1} phenolphthalein was dissolved in the pentanol, octanol and DEP – it was found to have a low solubility in octanoic acid. Note that deprotonated phenolphthalein will have a higher aqueous solubility than the neutral form and that phenolphthalein may cross the phase boundary without oil or water also crossing the boundary.

^{1}H NMR Spectroscopic Studies

For the ^{1}H NMR spectroscopic studies, 3.5 mL of 20 mM TTAB (pH = c. 13) was placed in a glass vial. To this was added 4 × 4 µL droplets of the given oil formulation. After 1 minute, 1 mL of the lower part of the aqueous phase was sampled at a mid-radius, taking great care not to sample any oil phase droplets. This sample was then homogenised and 600 µL used for ^{1}H NMR spectroscopy. All NMR measurements were performed using a two-channel Bruker Avance III HD 600 spectrometer equipped with a 5-mm BBFO probehead operating at 600.1 MHz for 1H. The ^{1}H chemical shifts are reported relative to TTAB at δ = 3.13 ($RN^+(CH_3)_3$, 9H, s). For acquisition of quantitative ^{1}H solvent-suppressed experiments, standard presaturation sequence (zgpr from Bruker pulse program library) was used. Temperature was regulated at 298 K. Each spectrum was acquired in 4 scans. CW presaturation (1 mW) was applied on resonance during relaxation delay (2 s).

In order to evaluate the best performing suppression sequence some preliminary tests using internal standard with known concentration were performed. Selective excitation water suppression sequences (W5-WATERGATE and PURGE) demonstrated strong artefacts on multiplets in the spectrum due to J-modulation. T1-based suppression sequence (1D-NOESY) demonstrated results comparable to presaturation terms of quantification reproducibility, although, the latter was chosen to avoid influence of variable T1 relaxation rates for different protons in the sample. All spectra were processed on a Windows workstation using the TOPSPIN 3.2 software package.

Each sample was run in triplicate using 5 mM maleic $acid_{(aq)}$ as an internal standard, present within a capillary inset within the NMR tube. Chemical shift regions corresponding to each of the oils were integrated manually, using a baseline correction method. Baseline correction was used as solvent suppression sometimes led to a variable baseline, which, coupled

with the small nature of the peaks of interest, would otherwise lead to large errors in the measured values. The values were then corrected by subtracting the mean value found for blanks, which corresponded to the single / binary oil combinations not containing the oil of interest. This was again done to counter factors such as baseline variation and noise, present again due to the small nature of the peaks of interest, both compared to the noise and to the much larger TTAB peaks, and the effect of solvent suppression on the baseline. Supplementary Figures 1-4 show a representative ^{1}H NMR spectrum for this analysis, in this case for the static-1 sample.

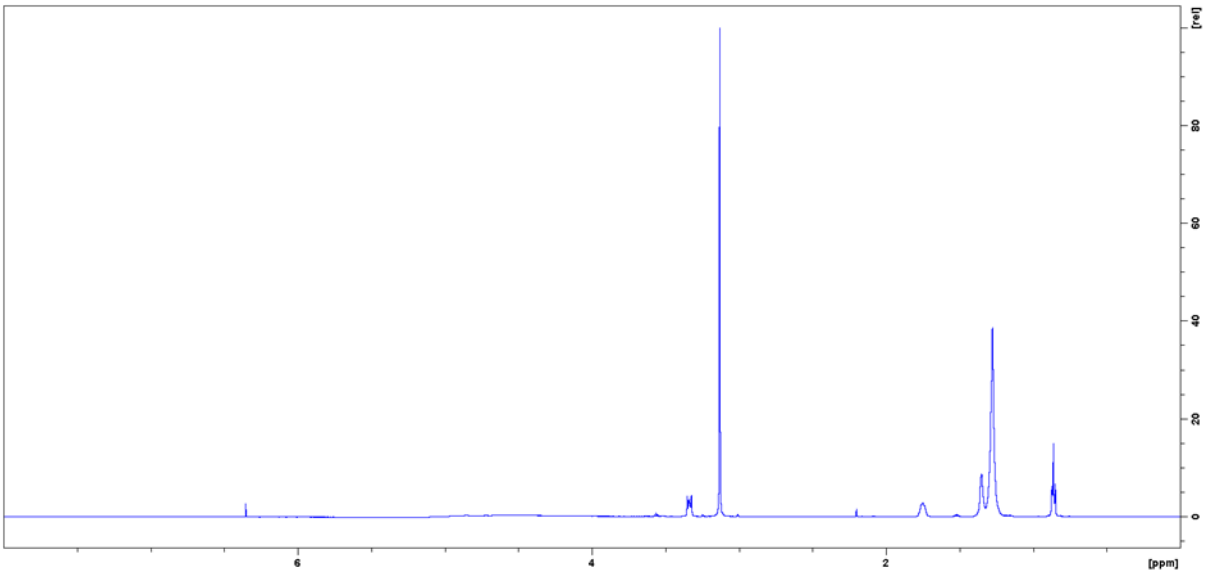

*Supplementary Figure 1 – The ^{1}H NMR spectrum for the static-1 sample. Most obvious are the TTAB peaks, which are assigned as follows: ^{1}H NMR (600 MHz, H_2O) δ 3.34 (2H, m, RC**H**$_2$($N^+(CH_3)_3$), 3.13 (9H, s, $RN^+(C$**H**$_3)_3$), 1.75 (2H, m, RC**H**$_2CH_2(N^+(CH_3)_3$), 1.17-1.41 (22H, m, chain C**H**$_2$), 0.86 (3H, t, terminal C**H**$_3$).*

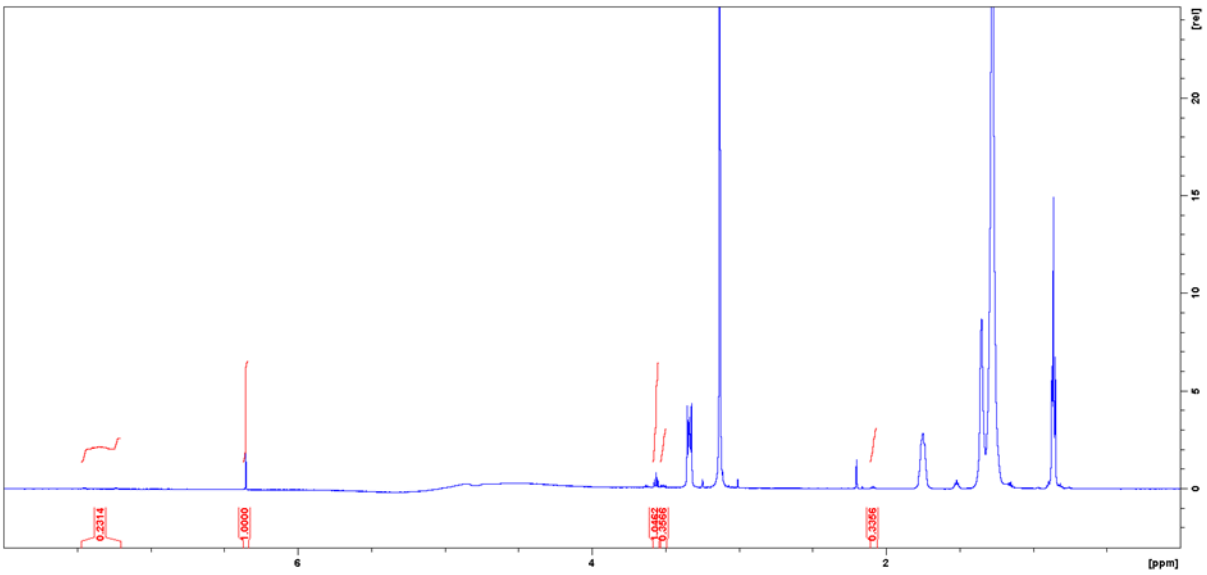

Supplementary Figure 2 – A higher magnification of the ^{1}H NMR spectrum for the static-1 sample, with the integrals of oil peaks of interest shown. The singlet at δ = 2.20 corresponds to residual acetone from the washing process and does not affect quantitative analysis. Baseline deviation around the supressed water peak (δ = 4.0-6.0) can also be seen. The peak at δ = 1.52 corresponds to a mixture of the oils and is not used for analysis.

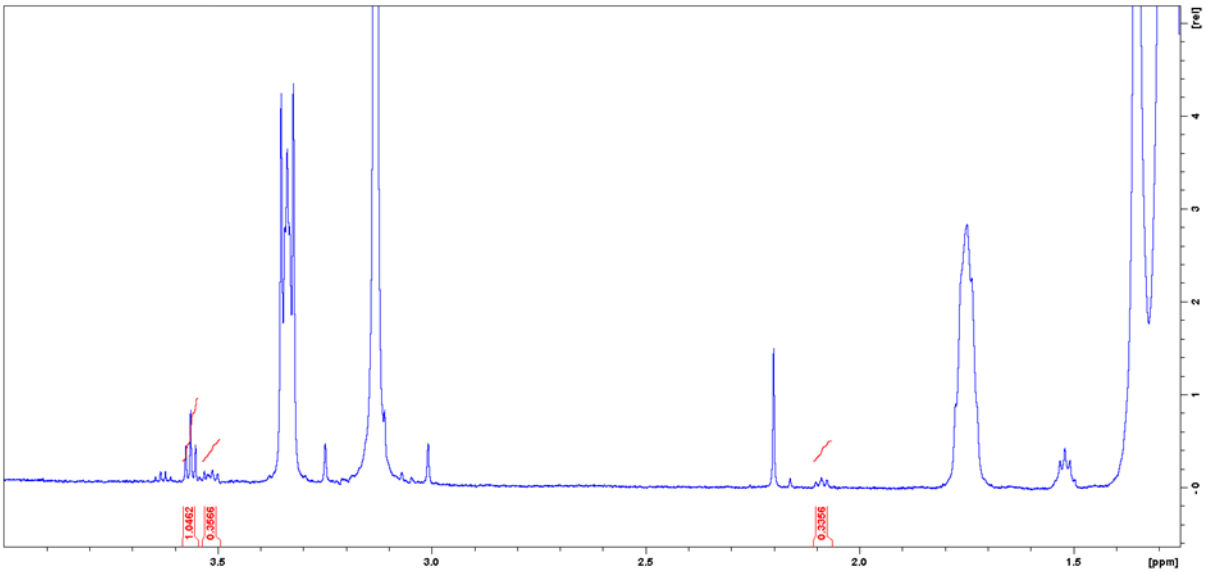

Supplementary Figure 3 - A higher magnification of the ^{1}H NMR spectrum for the static-1 sample, in which can be seen the integrated peaks for octanoic acid (δ = 2.09, t), octanol (δ = 3.51, t), pentanol (δ = 3.56, t) and ethanol (δ = 3.63, q), formed by DEP hydrolysis.

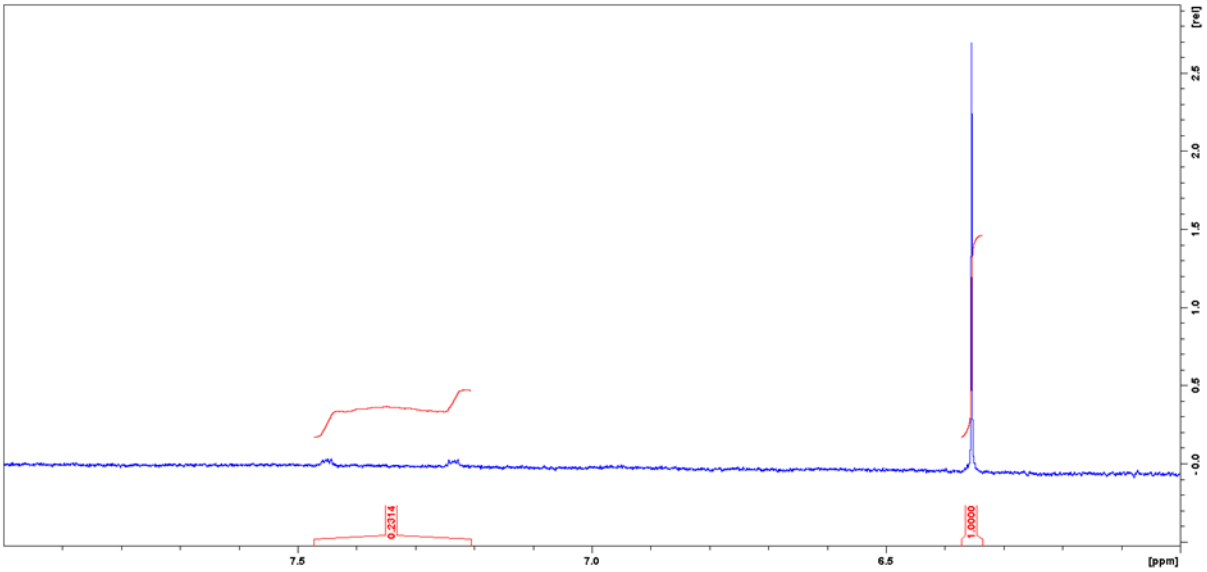

Supplementary Figure 4 - A higher magnification of the ^{1}H NMR spectrum for the static-1 sample, in which can be seen the integrated peaks for DEP (δ = 7.21-7.47, m) and the maleic acid internal standard (δ = 6.35, s).

The formulations used to produce Figure 3 are as shown in Supplementary Table 3:

Formulation	Observed Behaviour	TTAB	1-Octanol	1-Pentanol	DEP	Octanoic Acid
Vib-1	High vibration fitness	100	18.1	2.1	60.1	19.7
Vib-2	High vibration fitness	100	41.9	23.1	19.9	15.2
Vib-3	High vibration fitness	100	8.4	2.3	73.7	15.6
LoVib-1	Low vibration fitness	100	46.5	33.1	0.1	20.4
LoVib-2	Low vibration fitness	100	14.3	14.7	16.3	54.8
LoVib-3	Low vibration fitness	100	0.5	3.3	65.5	30.8
Div-1	High division fitness	100	36.3	18.2	41.4	4.2
Div-2	High division fitness	100	30.8	15.4	50.3	3.5
4Drop-1	Division fitness = 4 4 droplet present after 1 minute	100	28.1	12.2	19.8	39.9
4Drop-2	Division fitness = 4 4 droplet present after 1 minute	100	42.5	17.1	27.4	13.0

LoDiv-1	Low division fitness	100	29.1	58.3	5.9	6.6
LoDiv-2	Low division fitness	100	60.6	4.5	28.8	60.9
LoDiv-3	Low division fitness	100	28.9	39.8	22.2	9.1
Stat-1	Low movement fitness (Static droplets)	100	27.1	10.1	60.9	1.9
Stat-2	Low movement fitness (Static droplets)	100	59.2	6.7	29.5	4.7
Mov-1	High movement fitness	100	20.4	56.0	20.8	2.7
Mov-2	High movement fitness	100	46.0	17.7	32.4	3.6
Mov-3	High movement fitness	100	20.4	45.1	20.9	13.6

Supplementary Table 3 - Droplet formulations used in experiments carried out for the NMR study

Robotic Procedures

All automated experiments were undertaken at 24 ± 2 °C within a fumehood.

General Experimental Procedure:

1. Start experiment
2. Move carriage to dish and dispense surfactants
3. Move carriage to oil-mixing rack and dispense oils
4. Mix oils via magnetic stirrer
5. Aspirate oil mixture using syringe
6. Move carriage to dish and lower syringe to just above aqueous phase surface
7. Dispense four droplets in a square configuration
8. Move white screen over dish
9. Record 1 minute video of droplets
10. Empty and clean dish

Cleaning Procedures:

During proximity limited random search:

1. Move to dish
2. Dispense 5.8 mL acetone
3. Clean syringe
4. Empty dish
5. Repeat 1-4 with 7.5 mL acetone
6. Move 6-way valves to ‘water’
7. Dispense 1 ml water from both aqueous pumps
8. Move 6-way valves to ‘air’
9. Dispense 2.2 mL air
10. Empty dish, including side
11. Repeat 6-9 with 2 mL water
12. Clean syringe
13. Empty dish
14. Repeat 5, emptying side of dish
15. Home carriage
16. Aerate syringe

During genetic algorithm led exploration:

1. Move to dish
2. Dispense 5.8 mL acetone
3. Clean syringe
4. Empty dish
5. Repeat 1-4 with 7.5 mL acetone
6. Dispense 4 ml water
7. Empty dish including side
8. Dispense 4 ml water
9. Clean syringe
10. Empty dish
11. Repeat 5, emptying side of dish
12. Home carriage
13. Aerate syringe

Supplementary Discussion

There are two rather unexpected observations that have been made for many droplet recipes – that the droplets often change colour from red to purple and the appearance of a white precipitate from the oil droplets. It was suspected that the white material ejected from droplets was due to octanoic acid precipitating out with the TTAB. To confirm this, each (undyed) oil was mixed with the aqueous phase. For octanoic acid an opaque, white suspension was obtained, whilst two clear layers were observed for all of the other oils, despite vigorous shaking. This confirmed that it is the octanoic acid that causes the white precipitate. The dye used for the oil droplets, Sudan III, contains a phenol moiety, with the slightly acidic OH oxygen conjugated to the extended azo structure. If and when the dye is mixed with the very basic aqueous phase, this will be deprotonated, which explains the colour change from red to purple as a higher wavelength will be absorbed. This was confirmed by mixing each of the dyed oils with the basic aqueous phase in bulk. The red-purple colour change was observed for all four oils, although it was slightly slower with octanoic acid, and this could be reversed by the addition of an excess of aqueous acid, thus reprotonating the dye.

Supplementary Figures

Supplementary Figure 5 shows how the predicted density and dynamic viscosity compare to the measured density and dynamic viscosity for various oil formulations. For the predicted density a simple weighted average was used,[3] thus assuming ideal solutions. For the prediction of dynamic viscosity the Arrhenius equation was used:[4]

$$\mu_{mix} = e^{x_i ln\mu_i + x_j ln\mu_j \ldots}$$

Where x = mole fraction of oil and μ is the viscosity of the mixture or pure oil. Thus ideal solutions are assumed in both cases. The densities and viscosities of the pure oils used are shown in Supplementary Table 5.

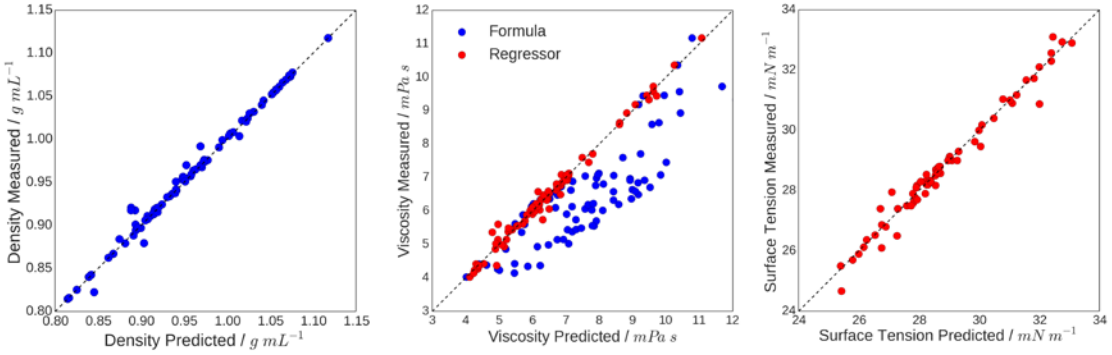

Supplementary Figure 5 – Plots of the predicted density (left), dynamic viscosity (centre) and surface tension (right) against their measured values. Blue points at predicted using weighted mean (density) and Arrhenius based method (viscosity) whilst red values are predicted using an SVM regressor. This is a reproduction of Figure 2 in the main paper, reproduced here for clarity.

As can be seen from Supplementary Figure 5, the predicted density matches the measured density very well when using the weighted mean. For viscosity, however, there are significant differences, with predicted viscosities being higher than the measured viscosities. There is also no satisfactory method for the prediction of the surface tension of mixtures. Hence, for viscosity and surface tension, we trained a SVM regressor using a 'RBF' kernel with parameters C and γ selected using 10 fold cross-validation using a mean squared error cost function to enable their prediction.

The selected parameters were $C = 100$ and $\gamma = 100$ for viscosity and $C = 100$ and $\gamma = 10^{-0.2}$ for surface tension.

From the resultant dataset of predicted densities, dynamic viscosities and surface tensions, another SVM regressor algorithm was used to subsequently predict the oil behaviours. A SVM regressor using a 'RBF' kernel was trained with C and gamma selected using 10 fold cross-validation with a mean squared error cost function to enable their prediction.

The selected parameters were $C = 100$ and $\gamma = 1$ for division and vibration and $C = 100$ and $\gamma = 0.1$ for movement.

Supplementary Figure 6 shows the predicted vibration, movement and division data plotted against the formulation physical properties, in the same manner as for Figure 4. The behavioural trends are seen to be consistent with the experimental data, thus showing how it is now possible to predict droplet behaviour from oil formulation, via the prediction of the formulation density, dynamic viscosity and surface tension.

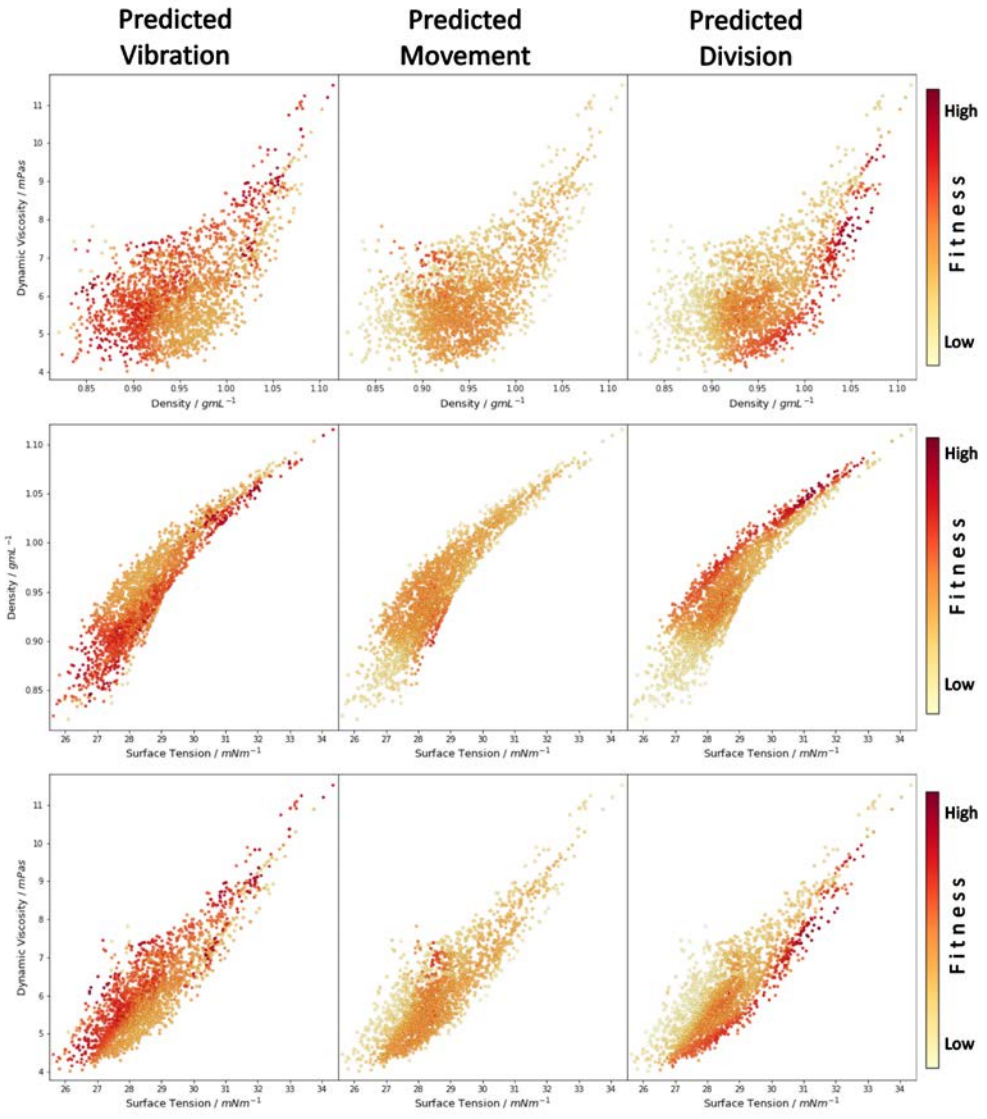

Supplementary Figure 6 - Impact of dynamic viscosity, density and surface tension on droplet behaviour: movement (left), vibration (centre) and division (right). Each dot is an experiment, the colour is proportional to the intensity of the behaviour as predicted by our machine learning model.

From a video showing swarming behaviour (Aqueous phase: 4.4 % TTAB, 14.8 % CTAB, 20.8% Triton X-100, 39.3 % PEG-400, 14.4 % DDMAB, 6.3 % Brij-O10, Oil phase: 3.5 % 1-Octanol. 56.1 % 1-pentanol, 33.9 % DEP, 9.7 % Octanoic acid), frames were taken from 20, 40, 60, 80, 100, 110

and 120 s. These frames were analysed using an ImageJ[5] macro to count the number of droplets and tabulate their coordinates in the frame:

```
//setTool("oval");
makeOval(113, 19, 421, 424);
run("Crop");
setBackgroundColor(255, 255, 255);
run("Clear Outside");
run("8-bit");
setAutoThreshold("Default");
//run("Threshold...");
setOption("BlackBackground", true);
run("Convert to Mask");
run("Find Edges");
saveAs("PNG", FILE_PATH);
makeOval(6, 14, 411, 405);
run("Analyze Particles...", "size=2-80 show=Outlines display exclude summarize in_situ");
```

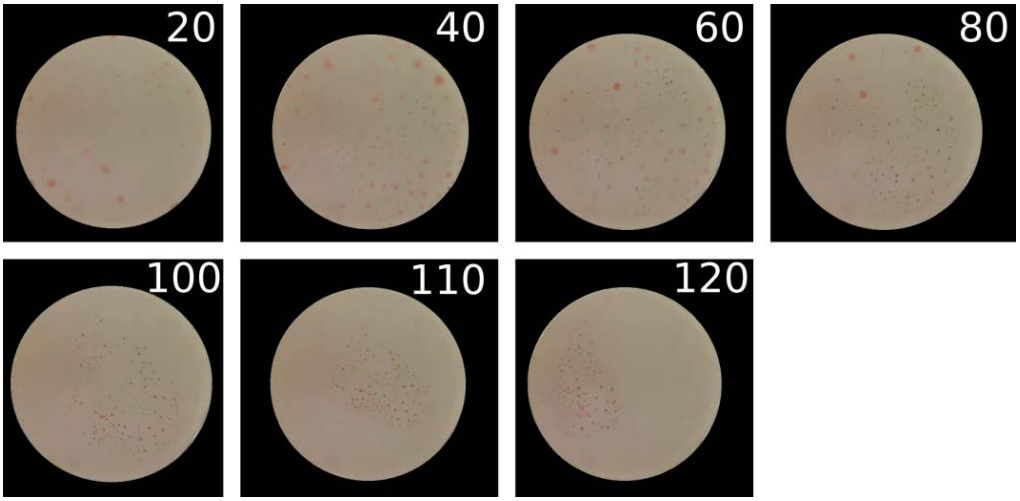

Supplementary Figure 7 – Snapshots from swarming video used for analysis of droplet position, along with their times at which they were taken in seconds.

From these droplet coordinates exported from ImageJ, the Euclidean distance was calculated between every droplet pair for each frame, which could be plotted as a histogram (Supplementary Figure 8). The mean inter-droplet distance was also computed, along with the standard deviation in this value, allowing a Gaussian fit to be estimated for each histogram, as in Figure 6. This standard deviation gives a sense of the range of inter-droplet distances.

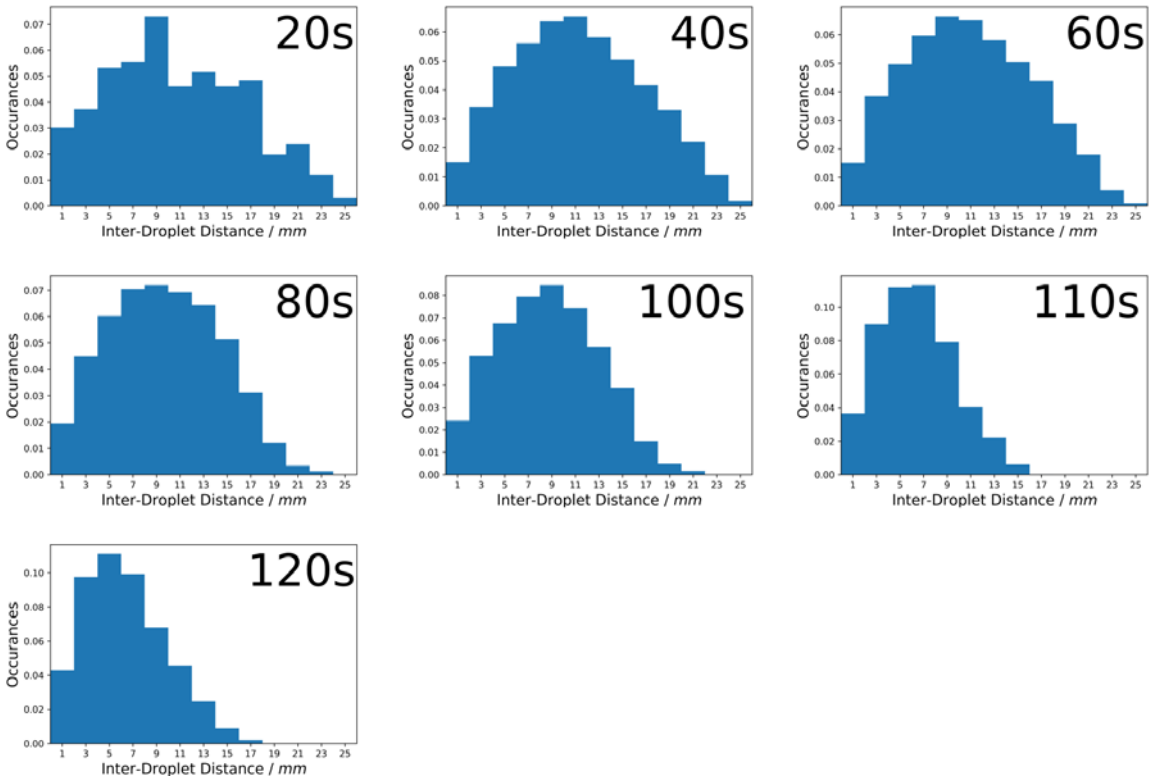

Supplementary Figure 8 - Histograms showing the inter-droplet distances for a swarming formulation – as for Figure 6.

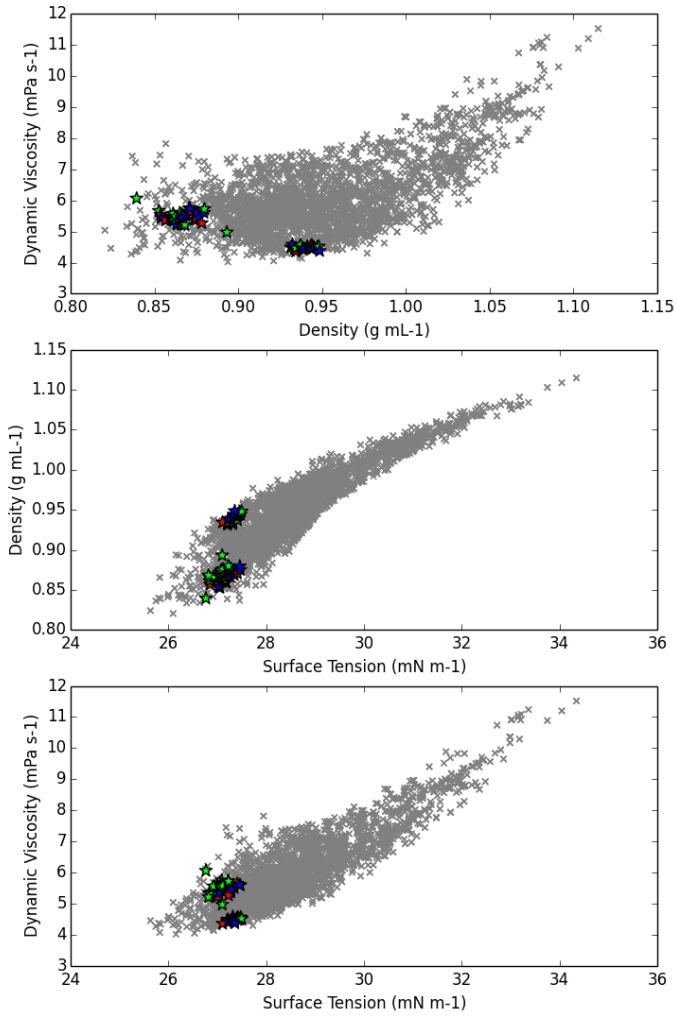

Supplementary Figure 9- Swarming regions discovered from the random matrix screen and from indicator experiments, further explored by sampling formulations with similar predicted physical properties. The region at density = 0.925-0.960, viscosity = 4.25-4.30 and surface tension = 26.0 -27.5 corresponds to similar properties to swarming formulations found in the random matrix screen, while the region at density = 0.85-0.88, viscosity = 5.20-5.80 and surface tension = 26.8-27.1 describes formulations similar to those found among the pH indicator experiments. Green markers indicate formulations that exhibited swarming in both repeats, blue indicates that swarming was observed in one of the two, and red indicates that swarming was not observed in either repeat.

The GA run with 6 surfactants quickly discarded 2 surfactants (Brij and CTAB) for movement behaviour. It can be seen from Supplementary Figure 10 that over the course of the GA the fractions that these surfactants contributed to the formulations decreased to zero:

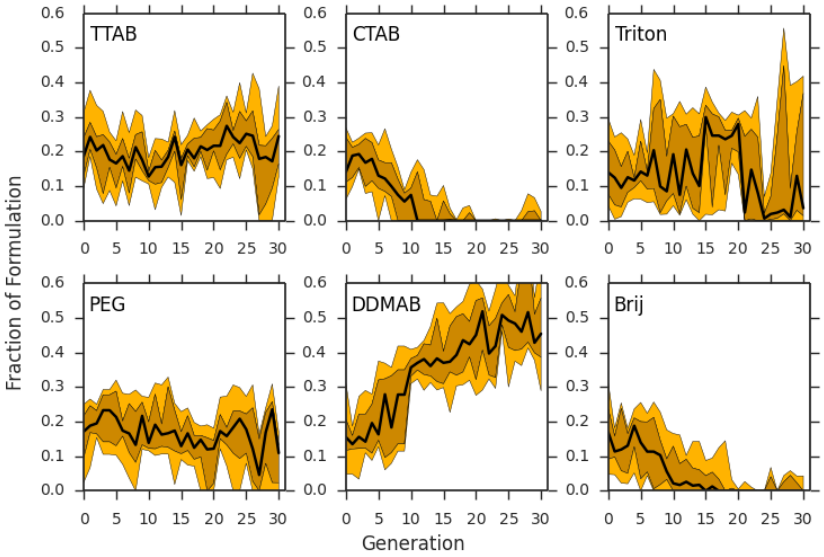

Supplementary Figure 10 - Fraction of formulation of one 30 generation genetic algorithm experimental run using six surfactant solutions. The same oil formulation was used for every experiment, optimised for movement. Experiments were repeated in duplicate. The black line represents the median for each generation, dark orange represents the distribution between upper and lower 25th percentile, and light orange represents the distribution between upper and lower 10th percentile.

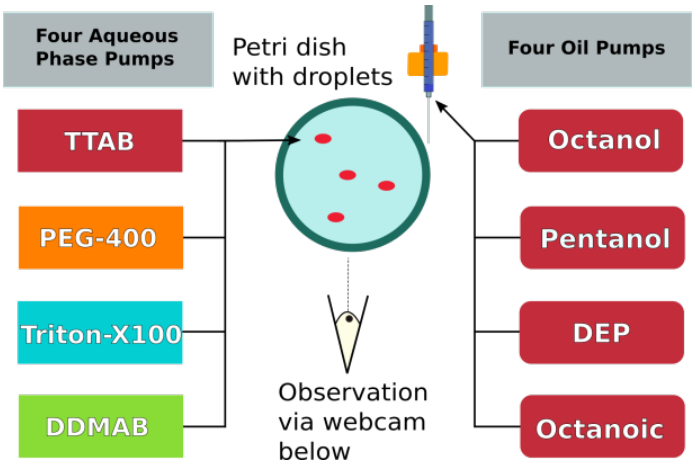

Supplementary Figure 11 - A schematic of the setup of the robotic assistant for the four aqueous, four oil phase experiments.

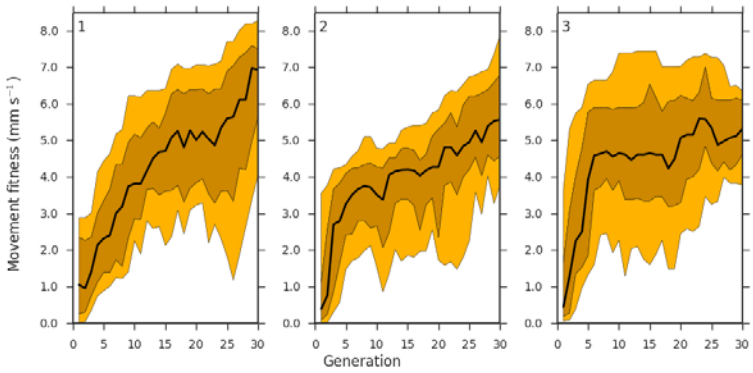

Supplementary Figure 12- Fitness vs Generation for each of the three runs of the four oil four aqueous phase optimisation. The black line corresponds to the median for each generation, the dark yellow area shows the distribution between the 75th and 25th percentile, and the pale yellow area shows the distribution between the 90th and the 10th percentile.

Supplementary Figure 13 shows the evolution of the composition of both the aqueous and oil phases during the evolutionary experiments. Despite similar upward trends in fitness across all three repeats of the optimisation, significant variations in compositional trends were seen between repeats. For example, the fraction of Triton-X100 remains steady at ≈0.3 in two repeats, but increases sharply from 0.24-0.49 within ten generations in the third repeat. The fraction of PEG-400 decreases to 0.02 and 0.12 in two repeats, but increases slightly from 0.23 to 0.25 in another. For DDMAB, the proportion increases to 0.35, remains constant at c. 0.25 and decreases to 0.09 across the three repeats. The median TTAB fraction rises slightly from around 0.20 to 0.23-0.30 for all repeats. For the oil phase, final octanol concentrations vary considerably, from 0.13-0.41, with its quantity falling in one optimisation and rising in another. Pentanol concentrations consistently fell from above 0.2 to 0.11 or below, whilst the total DEP concentration always rose. Overall, the compositional trajectories and final values differ significantly between runs while the upward trend in fitness is conserved, illustrating the complexity of the system and why it is beneficial to optimise the aqueous and oil phases together. Interestingly, as Supplementary Figure 14 shows, the physical properties of the oil phase are fairly consistent throughout the runs, despite this compositional variation.

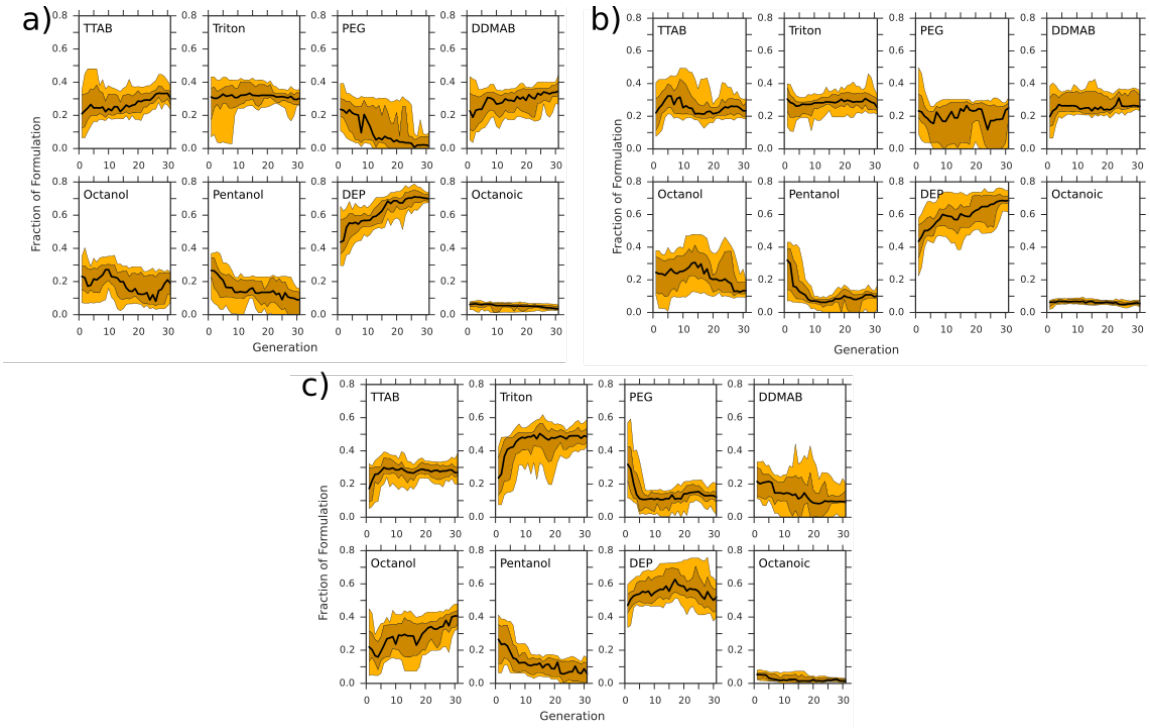

Supplementary Figure 13 - Fraction of oil formulation for three 30 generation genetic algorithm experimental runs using four surfactant solutions and four oils. Experiments were repeated in duplicate and optimised for movement. The black line represents the median for each generation, dark orange represents the distribution between upper and lower 25th percentile, and light orange represents the distribution between upper and lower 10th percentile.

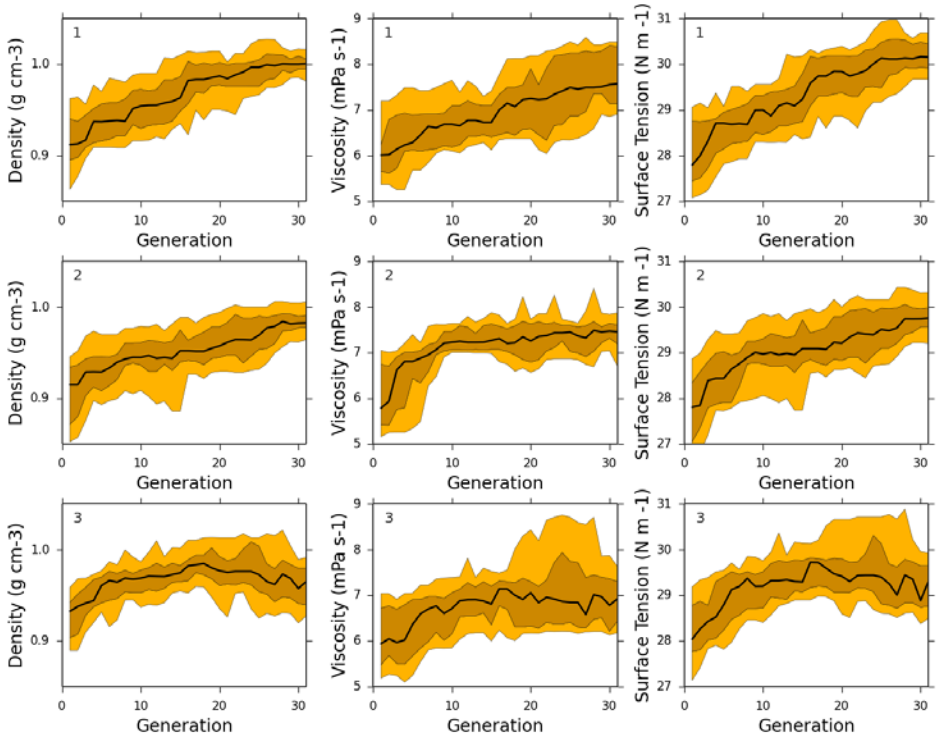

Supplementary Figure 14 - Physical properties vs Generation for the oil phase of the combined aqueous and oil phase optimizations. The black line represents the median for each generation, dark orange represents the distribution between upper and lower 25th percentile, and light orange represents the distribution between upper and lower 10th percentile.

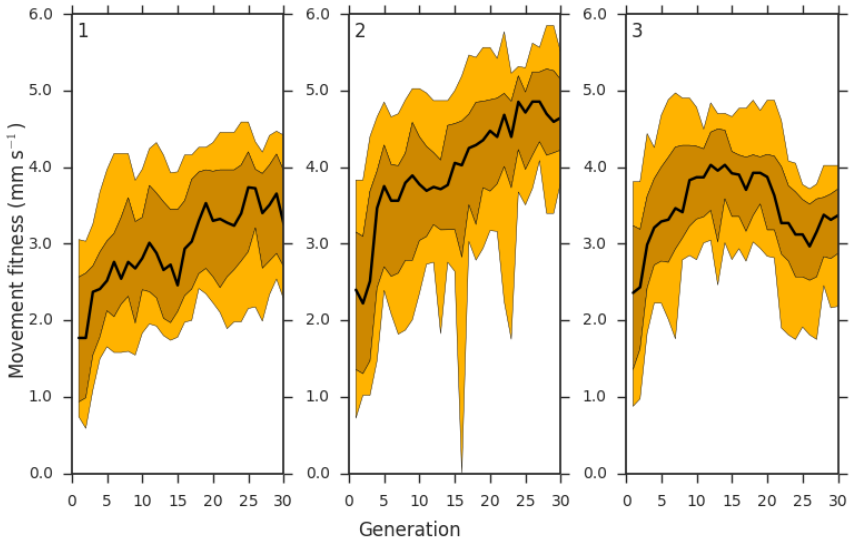

Supplementary Figure 15 - Fitness vs generation for aqueous phase only optimization, conducted in triplicate. The black line corresponds to the median for each generation, the dark yellow area shows the distribution between the 75th and 25th percentile, and the pale yellow area shows the distribution between the 90th and the 10th percentile.

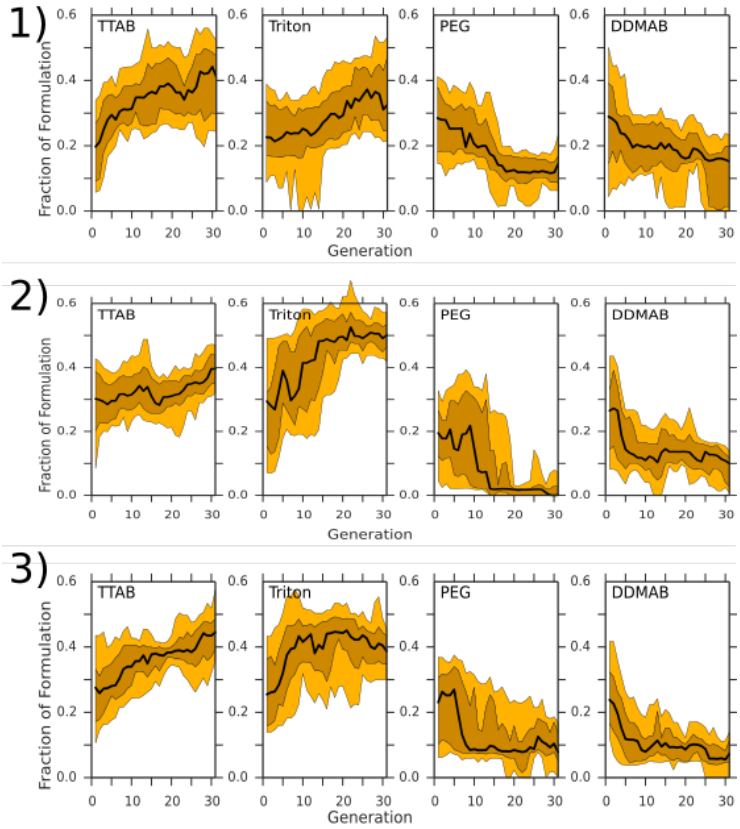

Supplementary Figure 16 - Formulation vs generation for the aqueous phase only optimization, conducted in triplicate. The black line corresponds to the median for each generation, the dark yellow area shows the distribution between the 75th and 25th percentile, and the pale yellow area shows the distribution between the 90th and the 10th percentile.

Supplementary Tables

Oil	**Water Solubility / *g L^{-1}***	**Molecular Weight g mol^{-1}**	**log P**	**Dipole Moment / D**	**Vapour Pressure (T / °C for 10 kPa pressure)**
1-octanol	0.46	130.23	3.07	1.76	128.2
1-pentanol	22	88.15	1.51	1.64	79.8
DEP	1.08	222.24	2.42	2.4	215.9
Octanoic Acid	0.68	144.21	3.05	1.15	165.5

Supplementary Table 4 - Some literature properties of the oils used in these experiments. The density, water solubility, surface tension and viscosity are from reference 1; the dipole moment and the vapour pressure are from reference;[6] *the logP values for 1-octanol and 1-pentanol are from reference*[7] *and for DEP and octanoic acid are from.* [6]

	Measured Properties				**Literature Properties**		
Oil	**Density / *g mL^{-1}***	**Surface Tension / *mN m^{-1}***	**Dynamic Viscosity / *mPa s^{-1}***	**Kinematic Viscosity / mm^2 s^{-1}**	**Density / *g mL^{-1}*, 20 °C**	**Surface Tension / *mN m^{-1}***	**Dynamic Viscosity / *mPa s^{-1}***

1-octanol	0.825	27.5	9.18	11.13	0.824	27.1	7.288
1-pentanol	0.815	25.5	4.03	4.94	0.811	25.4	3.619
DEP	1.118	35.9	12.87	11.52	1.12	19.6	10.625
Octanoic Acid	0.910	28.8	6.14	6.75	0.910	27.9	5.02

Supplementary Table 5 - The measured properties of the oils used for these experiments, with 0.25 mg mL-1 Sudan III dye. The literature density, surface tension and dynamic viscosity for the pure oils are from reference 1. Note that our experimental conditions do affect some of these values. Note especially the deviation of DEP's surface tension from the literature value – likely due to interaction with the aromatic dye.

Aqueous Phase (all 20 mM)	**Density / g mL^{-1}**	**Surface Tension / *mN m^{-1}***	**Dynamic Viscosity / *mPa s^{-1}***	**Kinematic Viscosity / mm^2 s^{-1}**
TTAB	1.0019	33.6	0.9946	0.9928
CTAB	0.9994	34.6	0.9882	0.9888
PEG-400	1.0106	53.1	1.043	1.032
Triton X-100	1.0005	31.4	1.015	1.014
Brij O-10	0.9995	31.9	1.057	1.058
DDMAB	1.0014	42.2	0.9950	0.9936

Supplementary Table 6 - Some measured properties of the aqueous phases used for robotic experiments.

TTAB	**CTAB**	**Triton**	**PEG 400**	**DD MAB**	**Brij-O10**	**1-Oct**	**1-Pent**	**DEP**	**Octanoic acid**	**Location**	**Behaviours**
3	12	23	23	17	19	41	5	28	24	walls	movement, division
3	12	23	23	17	19	41	5	28	24	walls	movement
35	10	7	12	31	2	0	33	35	29	middle	division, swarming, fusion
35	10	7	12	31	2	0	33	35	29	middle	division, swarming, fusion
22	22	22	8	23	1	8	45	35	10	some walls	explosion, swarming, fusion
22	22	22	8	23	1	8	45	35	10	some walls	explosion, swarming, fusion

Supplementary Table 7 - Sample random matrix experiment table.

	TTAB	**Triton**	**PEG**	**DDMAB**	**1-Oct**	**1-Pent**	**DEP**	**20% Octanoic in DEP**	**Original Fitness (mm s-1)**	**Mean Fitness (8 Repeats) (mm s-1)**	**STDEV**
1a	0.294	0.338	0.000	0.367	0.260	0.000	0.524	0.216	5.214	4.780	0.392
1b	0.257	0.409	0.099	0.235	0.182	0.142	0.501	0.176	5.153	4.150	0.587
1c	0.331	0.297	0.000	0.372	0.237	0.000	0.598	0.164	5.138	4.086	0.916
1d	0.356	0.271	0.000	0.373	0.193	0.009	0.656	0.142	5.124	3.902	0.999
2a	0.284	0.290	0.146	0.281	0.144	0.126	0.520	0.210	4.912	3.556	0.785
2b	0.305	0.328	0.000	0.368	0.124	0.108	0.488	0.280	4.822	4.578	0.446
2c	0.304	0.311	0.037	0.348	0.188	0.089	0.460	0.263	4.648	4.017	0.627
2d	0.234	0.208	0.150	0.408	0.160	0.098	0.444	0.297	4.624	1.122	0.706

3a	0.261	0.578	0.161	0.000	0.450	0.061	0.471	0.017	5.388	3.497	1.034
3b	0.261	0.451	0.107	0.181	0.440	0.028	0.432	0.100	4.711	3.911	0.790
3c	0.236	0.467	0.092	0.204	0.387	0.130	0.357	0.126	4.605	3.889	0.659
3d	0.354	0.569	0.053	0.024	0.358	0.040	0.533	0.069	4.270	3.026	0.320

Supplementary Table 8 - Formulations reproduced from the 8 parameter genetic algorithm optimization.

	TTAB	**Triton**	**PEG400**	**DDMAB**	**Original Fitness (mm s^{-1})**	**Mean fitness (8 repeats) (mm s^{-1})**	**STDEV**
1a	0.239	0.471	0.097	0.193	6.010	2.200	1.467
1b	0.517	0.474	0.000	0.009	5.444	3.524	0.840
1c	0.238	0.562	0.000	0.200	5.339	1.606	0.674
1d	0.246	0.493	0.060	0.201	5.197	4.087	0.871
2a	0.401	0.492	0.000	0.107	7.215	3.597	0.504
2b	0.384	0.496	0.021	0.099	6.625	3.403	1.063
2c	0.348	0.534	0.000	0.118	6.625	2.746	0.303
2d	0.357	0.574	0.000	0.069	6.552	3.196	1.334
3a	0.367	0.495	0.036	0.101	5.787	3.255	0.902
3b	0.215	0.556	0.075	0.154	5.358	1.662	1.225
3c	0.438	0.459	0.000	0.103	5.303	3.339	0.796
3d	0.348	0.489	0.080	0.084	5.280	3.448	0.170

Supplementary Table 9 - Formulations reproduced from the aqueous phase only genetic algorithm optimization.

Supplementary Videos

1. Supplementary Video 1 shows the 3-Dimensional versions of Figure 2. The density, surface tension and dynamic viscosity, predicted as described at Supplementary Figure 5, are plotted for the recipes previously tested, with the colour of the datapoint representing the fitness of the droplets in that experiment. This is plotted for the measured (left) and predicted (right) droplet fitness, with yellow representing low fitness and red high fitness. From these plots the physical property-fitness trends can easily be seen, as can the ability of the model to predict the overall behavioural trends.
2. Supplementary Video 2 shows single oil and binary oil formulations dyed with phenolphthalein. In this video you can see how the different oils behave differently, for example, pentanol goes very pink, has rapid flows and dissolves, whilst DEP only goes pink at the interface.
3. Supplementary Video 3 shows the same recipes (given in the following table) dyed with either Sudan III dye (red, left, as used for automated experiments) or phenolphthalein (pink at high pH, right).
    a) The droplets can be seen to drift around and seem to interact via white and pink material tethers. This leads to low activity droplets staying in close proximity and a number of fusion events. It is interesting to note how the pink material is only expelled in distinct directions, with no broader ‘clouds’ being released.
    b) The droplets can be seen to be moving quite smoothly throughout, often in a curved manner punctuated by brief pauses in between movement, often at the edge of the dish. It is interesting to note that there appears to be very little phase mixing – the oil droplets stay clear throughout the indicator video. The droplets are also seen to bump into one another on several occasions – implying that, in this case, fusion itself is disfavoured rather than the close proximity of droplets itself.
    c) The droplets are seen to massively divide in the initial stages of the video to give many small, unstable droplets. These then drift to the side where they undergo further fusion and division, leading to no active droplets at the end of the video. It is interesting to see how, in the indicator video, the droplets appear to influence one another’s movement. The high level of phase mixing is shown by the pink staining of both the oil and aqueous phases in the indicator video and by the pink colouration in the dye video due to deprotonation of the Sudan III dye.
    d) Low movement is observed in this video, as for the most part all the droplets are stuck to the edge of the dish. We also see the gentle expulsion of material from the indicator droplets and slow flows in the droplets which influence their movement.

e) For this low division fitness recipe, we observe the droplets moving straight to the edge of the dish, thus giving an active droplet count of 0. Interestingly, when at the edge of the dish, the droplets appear to wobble and expel material – showing how the apparently inactive droplets of the dye video are actually actively expelling material.

f) In this video we see classic swarming behaviour. Initially, we have massive division, which is followed by the collective movement of the small droplets and their rapid fusion to form larger droplets, before they stick to the side. It is interesting to see how the droplets appear to interact via their pink clouds, often following the same path to the edge of the dish. It is important to note that fusion does not always occur as rapidly for swarming as it does in this video.

g) In this video, the droplets are initially relatively inactive, before they begin to move in fairly rapid spurts. It is apparent from the indicator video that, during this initial lower activity phase, the droplets are actually expelling material. It could be that once this material is expelled the oil phase is more optimal for movement, or that the dissolution of the oil in the aqueous influences the surface tension such that movement is promoted. For example, the material could be inhomogeneously dissolved, leading the surface tension variations and the promotion of Marangoni instabilities, leading to the variable droplet movement observed.

h) In this video the droplets are seen to be stationary, stuck to the side. There appears to be no oil-aqueous phase mixing, as evidenced by the lack of any pink colouration.

Formulation / %	TTAB	1-Octanol	1-Pentanol	DEP	Octanoic Acid
A	100	18.1	2.1	60.1	19.7
B	100	30.8	15.4	50.3	3.5
C	100	28.9	39.8	22.2	9.1
D	100	59.2	6.7	29.5	4.7
E	100	60.6	4.5	28.8	6.1
F	100	20.4	45.1	20.9	13.6
G	100	27.1	10.1	60.9	1.9
H	100	41.9	23.1	19.9	15.2

Supplementary Table 10 - Formulations shown in Supplementary Video 1.

4. Supplementary Video 4 shows the operation of the platform.
5. Supplementary Video 5 shows the observed droplet behaviours: Movement, division, vibration, fusion, pulsing, and swarming. Videos correspond to the recipes shown in Supplementary Table 11

Formulation / %	TTAB	CTAB	Triton X-100	PEG 400	DDMAB	Brij-O10	1-Oct	1-Pent	DEP	Octanoic acid
Movement	26.1	0	57.8	16.1	0	0	45.0	6.1	47.1	1.7
Division	7.3	0.2	9.1	50.0	30.0	1.6	20.3	20.8	57.8	1.2
Vibration	16.4	17.8	19.3	10.3	28.1	8.2	11.1	34.4	42.3	11.7
Fusion	0.0	0.0	0.0	0.0	0.0	100	0.0	0.0	100	0.0
Pulsing	34.2	21.6	6.9	14.5	16.7	6.1	17.5	28.9	33.3	20.1
Swarming	100.0	0.0	0.0	0.0	0.0	0.0	1.0	51.4	35.7	11.8

Supplementary Table 11 - Formulations used for the various behaviours in Supplementary Video 2.

6. Supplementary Video 6 shows the highest movement formulations from each genetic algorithm run – oil only, aqueous only and simultaneous aqueous and oil phase optimisation. Videos correspond to the recipes shown in Supplementary Table 12

Formulation / %	TTAB	CTAB	Triton X-100	PEG 400	DDMAB	Brij-O10	1-Oct	1-Pent	DEP	Octanoic acid
Oil Only	100	0	0	0	0	0	16.2	28.1	44.0	11.8
Aqueous Only	40.1	0	49.2	0.0	10.7	0	16.2	28.1	53.4	2.4
Oil and Aqueous	26.1	0	57.8	16.1	0	0	45.0	6.1	48.5	0.3

Supplementary Table 12 - Highest fitness formulations shown in Supplementary Video 3.

Supplementary References

1. Gutierrez, J. M. P., Hinkley, T., Taylor, J. W., Yanev, K. & Cronin, L. Evolution of oil droplets in a chemorobotic platform. *Nat. Commun.* **5,** 5571 (2014).

2. Gutierrez, J. M. P., Hinkley, T., Taylor, J. W. & Yanev, K. Hardware and Software manual for Evolution of Oil Droplets in a Chemorobotic Platform. *Arxiv* 1–42 (2014).

3. Khalil, M. I., Al-Yami, R. A. H. & Al-Khabbas, M. H. Introducing mole fraction in the density calculations of liquid-liquid solutions. *Int. J. Phys. Sci.* **8,** 27–30 (2013).

4. Zhmud, B. Viscosity Blending Equations. *Lube-Tech* **121,** 1–4 (2014).

5. Schneider, C. a, Rasband, W. S. & Eliceiri, K. W. NIH Image to ImageJ: 25 years of image analysis. *Nat. Methods* **9,** 671–675 (2012).

6. *CRC Handbook of Chemistry and Physics*. (CRC Press, 2005).

7. Sangster, J. Octanol-Water Partition Coefficients of Simple Organic Compounds. *Journal of Physical and Chemical Reference Data* **18,** 1111–1229 (1989).